Autophagy 9:8, 1214–1227; August 2013; © 2013 Landes Bioscience

IκB kinase complex (IKK) triggers detachment-induced autophagy in mammary epithelial cells independently of the PI3K-AKT-MTORC1 pathway

Nan Chen and Jayanta Debnath*

Department of Pathology and Helen Diller Family Comprehensive Cancer Center; University of California, San Francisco; San Francisco, CA USA

Keywords: autophagy, anoikis, extracellular matrix, integrin, mammary epithelial cells

Abbreviations: AKT, protein kinase B; CHUK/IKKα, conserved helix-loop-helix ubiquitous kinase/inhibitor of nuclear factor kappa-B kinase subunit α; ECM, extracellular matrix; GAP, GTPase activating protein; IKBKG, inhibitor of nuclear factor kappa-B kinase subunit gamma (IKKγ); ITGA3-ITGB1, α3β1 integrin; ITGA6-ITGB4, α6β4 integrin; IκB, inhibitors of NFKB; IκB-SR, IκB super-repressor; IKBKB/IKKβ, inhibitor of kappa light polypeptide gene enhancer in B-cells, kinase β/inhibitor of nuclear factor kappa-B kinase subunit β; LAMA5, laminin 5; MAP3K7/TAK1, mitogen-activated protein kinase kinase kinase 7/transforming growth factor-β-activated kinase 1; MEC, mammary epithelial cells; MTORC1, mammalian target of rapamycin complex 1; NFKB, nuclear factor kappa B; MEFs, mouse embryonic fibroblasts; PI3K, phosphoinositide 3-kinase; rBM, reconstituted basement membrane; 3D culture, three-dimensional culture; RHEB, Ras homolog enriched in brain; RPS6, ribosomal protein S6; TSC1, tuberous sclerosis complex 1 (hamartin); TSC2, tuberous sclerosis complex 2 (tuberin)

Adherent cells require proper integrin-mediated extracellular matrix (ECM) engagement for growth and survival; normal cells deprived of proper ECM contact undergo anoikis. At the same time, autophagy is induced as a survival pathway in both fibroblasts and epithelial cells upon ECM detachment. Here, we further define the intracellular signals that mediate detachment-induced autophagy and uncover an important role for the IκB kinase (IKK) complex in the induction of autophagy in mammary epithelial cells (MECs) deprived of ECM contact. Whereas the PI3K-AKT-MTORC1 pathway activation potently inhibits autophagy in ECM-detached fibroblasts, enforced activation of this pathway is not sufficient to suppress detachment-induced autophagy in MECs. Instead, inhibition of IKK, as well as its upstream regulator, MAP3K7/TAK1, significantly attenuates detachment-induced autophagy in MECs. Furthermore, function-blocking experiments corroborate that both IKK activation and autophagy induction result from decreased ITGA3-ITGB1 (α3β1 integrin) function. Finally, we demonstrate that pharmacological IKK inhibition enhances anoikis and accelerates luminal apoptosis during acinar morphogenesis in three-dimensional culture. Based on these results, we propose that the IKK complex functions as a key mediator of detachment-induced autophagy and anoikis resistance in epithelial cells.

Introduction

Extracellular matrix (ECM) interactions with integrin receptors play a critical role in cell proliferation, growth and survival. The detachment of cells from ECM disrupts integrin engagement and triggers programmed cell death, termed anoikis.[1,2] Anoikis prevents normal epithelial cells from colonizing in inappropriate ECM environments, thus maintaining tissue integrity. Studies of lumen formation in three-dimensional culture of mammary epithelial cells (MEC) reveal a critical role for anoikis in luminal clearance.[3] On the other hand, evidence also indicates that ECM detachment can trigger antiapoptotic signals, which presumably allow cells to survive for limited periods of time prior to reestablishing ECM contact.[1] Recent work demonstrates that the induction of autophagy, an evolutionally conserved lysosomal degradation process, serves as an important survival pathway during ECM detachment. Inhibiting autophagy enhances anoikis and accelerates luminal clearance in 3D mammary epithelial cultures.[4] Importantly, antibody-mediated blockade of ITGB1/integrin β1 function is sufficient to induce autophagy in attached cells, while the addition of a laminin-rich ECM abrogates autophagy in detached cells; collectively, these findings indicate that the loss of ECM-integrin receptor engagement directly mediates detachment-induced autophagy.[4]

Currently, the intracellular signals linking the loss of ECM-integrin receptor engagement to detachment-induced autophagy

*Correspondence to: Jayanta Debnath; Email: Jayanta.Debnath@ucsf.edu
Submitted: 12/19/12; Revised: 04/25/13; Accepted: 04/29/13
http://dx.doi.org/10.4161/auto.24870

remain poorly defined. In mammalian cells, multiple pathways regulate autophagy during starvation or stress; among these, the PI3K-AKT-MTORC1 pathway is the archetypal regulator of autophagy.[5] MTORC1 activity is inversely correlated with autophagy induction. Both nutrient starvation and growth factor withdrawal cause deactivation of the PI3K-AKT-MTORC1 pathway, resulting in the induction of autophagy. Furthermore, during ECM detachment, recent work suggests that activation of the endoplasmic reticulum (ER) kinase, EIF2AK3/PERK can promote autophagy via inhibition of the MTORC1 pathway.[6]

In addition to MTORC1, the nuclear factor kappa B (NFKB) signaling pathway has been implicated in both autophagy regulation as well as anoikis resistance.[7,8] The NFKB pathway is involved in the transcriptional control of multiple cellular functions, including cell proliferation, apoptosis, differentiation, inflammation and immune response. The IκB kinase (IKK) complex, the major regulator of the NFKB pathway, consists of two highly related catalytic subunits (CHUK/IKKα and IKBKB/IKKβ) and a regulatory subunit (IKBKG/IKKγ). In unstimulated cells, the NFKB proteins assemble inactive complexes with Inhibitors of NFKB/κB (IκB) proteins in the cytoplasm. Upon upstream kinases stimulation, IKK kinases phosphorylate the inhibitory molecule IκB, resulting in ubiquitination and degradation of IκB via proteasomes. Subsequently, the free NFKB dimers translocate to the nucleus and bind to κB sites on target genes, many of which are involved in stimulating inflammation, preventing apoptosis and enhancing cell proliferation.[9]

Notably, IKK can directly phosphorylate cellular proteins distinct from NFKB and IκB proteins, indicating that this kinase complex has biological functions beyond its canonical role in the NFKB pathway.[10] Remarkably, recent work has revealed a new link between IKK complex activation and autophagy induction via an NFKB independent mechanism; diverse autophagic stimuli activate the IKK complex and that IKK is required for optimal autophagy induction both in *vitro* and in *vivo*.[8] Importantly, IKK activation mediated autophagy induction can be uncoupled from NFKB activation. Consistent with these findings, both CHUK and IKBKB are required for starvation-induced autophagy; furthermore, IKK, but not NFKB, was critical for basal and starvation-induced autophagy gene expression.[11] Altogether, these findings suggest that autophagy can be regulated in an IKK-dependent, NFKB-independent manner in mammalian cells. Interestingly, IKBKB activity can also be downregulated by autophagic degradation, suggesting a complex interplay between autophagy and the IKK-NFKB pathway.[12,13]

In this study, we sought to delineate the intracellular signals necessary to induce autophagy in cells deprived of ECM contact. Whereas the PI3K-AKT-MTORC1 pathway is a major regulator of autophagy induction in detached mouse fibroblasts, the activation of IKK complex plays a key role in promoting autophagy in MECs deprived of ECM contact. We also demonstrated that the blockade of ITGA3-ITGB1 (α3β1 integrin) function is sufficient to activate IKK as well as induce autophagy in MECs. Moreover, pharmacological IKK inhibition enhances anoikis and accelerates luminal apoptosis during acinar morphogenesis in three-dimensional culture. Hence, we propose that the IKK complex functions as a key regulator of detachment-induced autophagy and anoikis resistance in specific cell types.

Results

Activation of the PI3K-AKT-MTORC1 pathway suppresses detachment-induced autophagy in mouse fibroblasts. A large body of work demonstrates that inactivation of MTORC1 plays an essential role in autophagy induction in response to diverse stimuli, including nutrient deprivation and loss of growth factor signals.[5] To assess if MTORC1 activity is reduced during ECM detachment, we cultured mouse embryonic fibroblasts (MEFs) and mammary epithelial cells (MCF10A) on poly-HEMA coated tissue culture dishes to prevent adhesion and monitored MTORC1 activity via the phosphorylation status of its well-defined downstream targets RPS6KB1 or RPS6.[14] In both cell types, we observed decreased MTORC1 activity in detached cells, which correlated with an increase in autophagic flux, evidenced by the increased turnover of the cleaved and phosphatidylethanolamine conjugated-form of LC3 (LC3-II) in the presence of the lysosomal cathepsin inhibitors E64d and pepstatin A (E/P) (**Fig. S1**).

As a result, we examined whether enforced MTORC1 activation during ECM detachment was sufficient to suppress autophagy. TSC1 and TSC2 form a complex to inactivate the RHEB GTPase, leading to inactivation of MTORC1. Cells lacking TSC2 exhibit deregulated hyperactivation of MTORC1.[15] Hence, we utilized *tsc2*$^{-/-}$ MEFs to test whether activation of MTORC1 suppresses autophagy induction during ECM detachment. *Tsc2*$^{+/+}$ or *tsc2*$^{-/-}$ MEFs were cultured attached or in suspension for 24 h to assay autophagic flux. Although increased LC3-II conversion and turnover was observed in suspended *Tsc2*$^{+/+}$ MEFs, LC3-II conversion and turnover were potently inhibited in *tsc2*$^{-/-}$ cells (**Fig. 1A**). To more rigorously validate these findings, we performed a rescue experiment and stably reintroduced either wild-type human TSC2 or a mutant version of TSC2^{N1643I} into *tsc2*$^{-/-}$ MEFs. TSC2^{N1643I} contains a point mutation in its GTPase activating protein (GAP) domain that abolishes the GAP activity toward RHEB, thereby rendering it unable to modulate MTORC1 activity. As shown in **Figure 1A**, wild-type TSC2 but not TSC2^{N1643I} rescued autophagy induction during ECM detachment in *tsc2*$^{-/-}$ MEFs. Importantly, the rescued autophagy induction also correlates with the ability of TSC2 to downregulate MTORC1 activity as monitored by RPS6 phosphorylation (**Fig. 1B**). These results support the idea that loss of MTORC1 activity functionally contributes to ECM detachment-induced autophagy in fibroblasts.

In response to growth factors, AKT directly phosphorylates multiple sites on TSC2 that suppress the inhibitory effect of TSC2 toward RHEB and MTORC1.[16,17] During ECM detachment, we also observed decreased AKT activity in suspended cells (**Fig. 1C**). To investigate whether AKT and its upstream regulator PI3K contribute to autophagy regulation during ECM detachment, we stably expressed activated forms of PIK3CA* (PIK3CA^{E545K}) and AKT (myrAKT) in wild-type MEFs. Cells

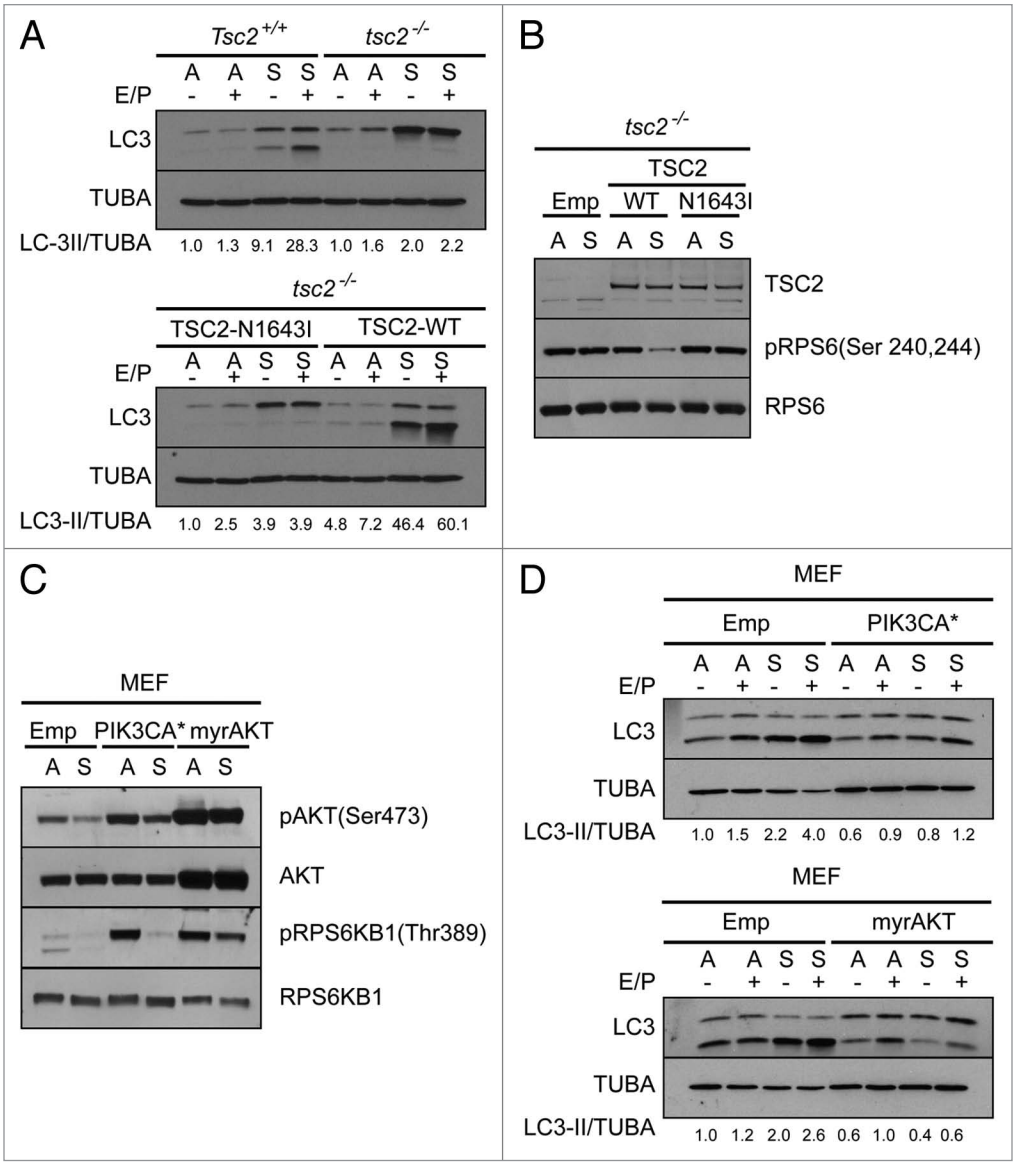

Figure 1. Activation of PI3K-AKT-MTORC1 pathway suppresses ECM detachment-induced autophagy in mouse embryonic fibroblasts (MEFs). (**A**) Top: Lysates from *Tsc2*$^{+/+}$ or *tsc2*$^{-/-}$ MEFs grown attached (A) or suspended (S) for 24 h were immunoblotted with anti-LC3 and anti-tubulin (TUBA) antibodies. Where indicated, E64d and pepstain A (E/P) were added 6 h prior to harvesting. Bottom: *tsc2*$^{-/-}$ MEFs stably expressing TSC2^{N1643I} or wild-type TSC2 (TSC2-WT) were grown attached or suspended for 24 h were immunoblotted with anti-LC3 and anti-TUBA antibodies. Where indicated, E64d and pepstain A (E/P) were added 6 h prior to harvesting. (**B**) Lysates from *tsc2*$^{-/-}$ MEFs stably expressing empty vector (Emp), TSC2-WT or TSC2^{N1643I} were grown attached (A) or in suspended (S) for 24 h were subject to immunoblotting with antibodies against TSC2, phospho-RPS6 ribosomal protein (Ser240,244) [pRPS6(Ser240,244)] and RPS6 ribosomal protein (RPS6). (**C**) Wild-type MEFs stably expressing empty vector (Emp), activated PIK3CA (PIK3CA*), or myristoylated AKT (myrAKT) were grown attached (A) or suspended (S) for 24 h. Cell lysates were subject to immunoblotting with antibodies against phospho-AKT(Ser473) [pAKT(Ser473)], AKT, phospho-p70 RPS6 Kinase(Thr389) [pRPS6KB1(Thr389)] or RPS6KB1. (**D**) Wild-type MEFs stably expressing empty vector (Emp) and PIK3CA* (top) or myrAKT (bottom) were grown attached (A) or suspended (S) for 24 h were immunoblotted with anti-LC3 and anti-TUBA antibodies. Where indicated, E64d and pepstain A (E/P) were added 6 h prior to harvesting.

expressing PIK3CA* and myrAKT exhibited higher levels of AKT and RPS6KB1 phosphorylation during both attachment and suspension, indicative of potently sustained activation of the AKT-MTORC1 pathway. At the same time, upon matrix detachment, LC3 conversion and LC3-II turnover were significantly reduced in PIK3CA* and myrAKT cells compared with empty vector controls (**Fig. 1D**). Together, these data corroborate that in fibroblasts, reduced activation of the PI3K-AKT-MTORC1 pathway plays a key role in autophagy induction during ECM detachment.

PI3K-AKT-MTORC1 activation does not inhibit autophagy in detached mammary epithelial cells. Next, we examined whether autophagy was regulated similarly in mammary epithelial cells. MCF10A cells were transfected with siRNA oligonucleotide pools targeting endogenous TSC2 and thereafter, grown attached or in suspension for 24 h. We confirmed

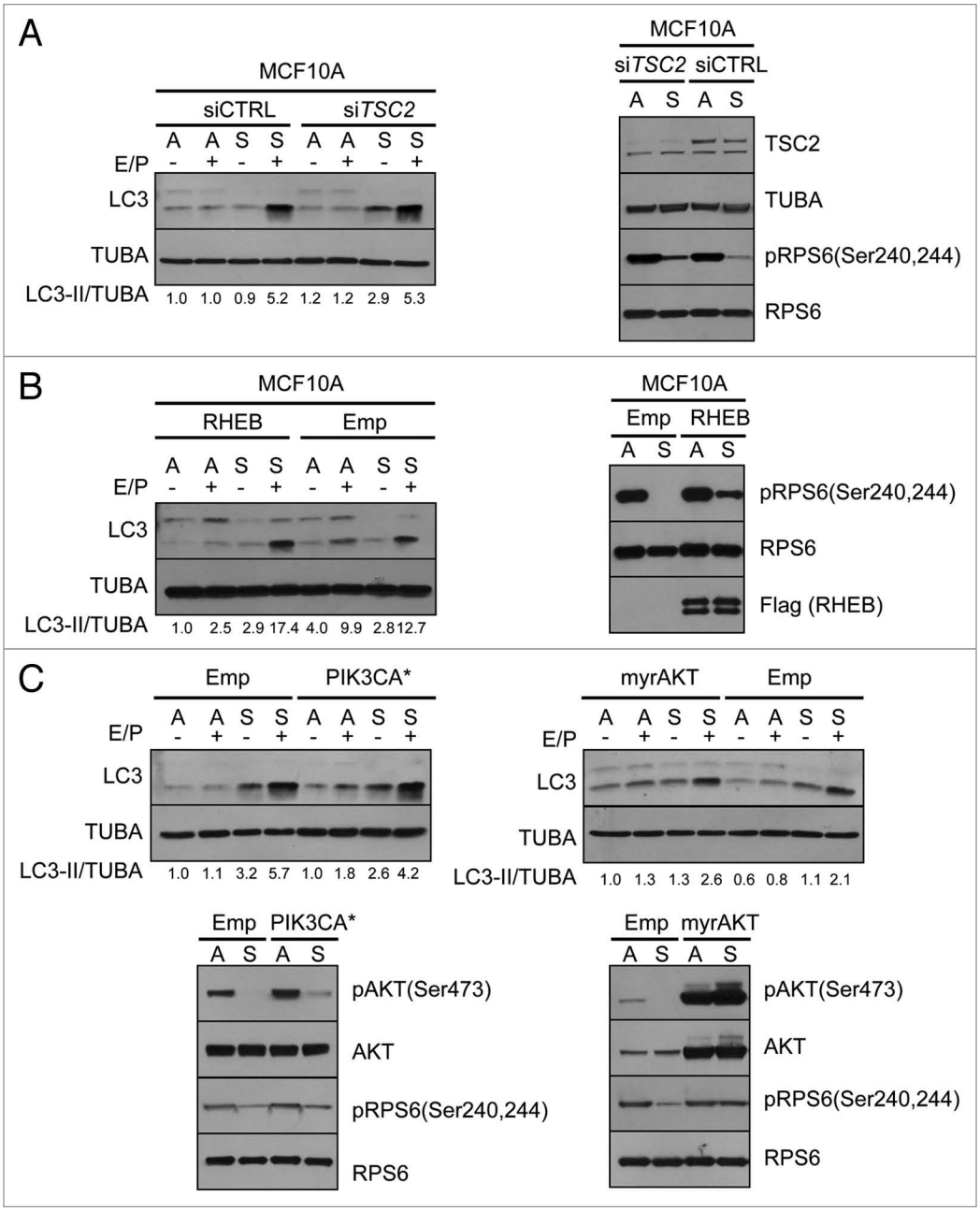

Figure 2. Activation of PI3K-AKT-MTORC1 pathway is not sufficient to suppress autophagy upon ECM detachment in mammary epithelial cells (MECs). (**A**) Left: MCF10A cells transfected with pooled nontargeting control (siCTRL) or siRNA against *TSC2* (si*TSC2*) were grown attached (A) or suspended (S) for 24 h were lysed and immunoblotted with anti-LC3 and anti-TUBA antibodies. Where indicated, E64d and pepstain A (E/P) were added to 6 h prior to harvesting. Right: Lysates from MCF10A cells transfected with siCTRL or si*TSC2* and then grown attached (A) or suspended (S) for 24 h were subject to immunoblotting with antibodies against TSC2, TUBA, pRPS6(Ser240,244) and RPS6. (**B**) Left: MCF10A cells stably expressing empty vector (Emp) or flag-tagged RHEB (RHEB) were grown attached (A) or suspended (S) for 24 h were lysed and immunoblotted with anti-LC3 and anti-TUBA antibodies. Where indicated, E64d and pepstain A (E/P) were added 6 h prior to harvesting. Right: Lysates from MCF10A cells stably expressing empty vector (Emp) or flag-tagged RHEB (RHEB) grown attached (A) or suspended (S) for 24 h were subject to immunoblotting with indicated antibodies. (**C**) Top: MCF10A cells stably expressing empty vector (Emp), PIK3CA* (left), or myrAKT (right) were grown attached (A) or suspended (S) for 24 h were lysed and immunoblotted with anti-LC3 and anti-TUBA antibodies. Where indicated, E64d and pepstain A (E/P) were added 6 h prior to harvesting. Bottom: MCF10A cells stably expressing empty vector (Emp), PIK3CA*, or myrAKT were grown attached or suspended for 24 h, lysed and immunoblotted with indicated antibodies.

efficient RNAi-mediated depletion of endogenous TSC2; moreover, TSC2 knockdown resulted in elevated RPS6 phosphorylation during detachment, in comparison to nontargeting control (siCTRL) cells (**Fig. 2A**). Nevertheless, we observed high levels of LC3 conversion and autophagic flux in si*TSC2* cells during substratum detachment (**Fig. 2A**). Because TSC2 depletion was

not sufficient to sustain RPS6 phosphorylation in detached cells to levels equivalent to attached controls, we construed that the residual levels of endogenous TSC2 in the RNAi-depleted cells were potentially sufficient to downregulate MTORC1 activity during detachment. Accordingly, we stably overexpressed RHEB to maintain MTORC1 activity.[18] Compared with control cells, a stronger phosphorylated RPS6 signal was detected in RHEB overexpressing cells in suspension. However, no significant decrease of LC3 conversion or autophagic flux in RHEB overexpressing cells was observed compared with empty vector control (Emp) (**Fig. 2B**). Since RPS6 phosphorylation was once again not fully restored to levels observed in attached cells, we speculated that other TSC2-RHEB-independent pathways also regulate MTORC1 activity during ECM detachment in MECs. For example, AKT1S1/PRAS40, a component of MTORC1 has been reported to inhibit RHEB-induced activation of the MTORC1 pathway.[19] On the other hand, AKT directly phosphorylates AKT1S1 and prevents its inhibition of MTORC1.[20] Hence, to scrutinize whether activation of the PI3K-AKT pathway was sufficient to maintain MTORC1 activity and suppress autophagy induction, we generated stable MCF10A cell lines expressing PIK3CA* or myrAKT. Nonetheless, upon ECM detachment, we did not detect any significant change on LC3 conversion or LC3-II flux in PIK3CA* or myrAKT cells compared with empty vector control (Emp) cells. Importantly, in myrAKT cells, detachment-induced autophagy was robustly induced, despite the fact that AKT and MTORC1 activation were fully sustained in detached cells to levels comparable to attached controls (**Fig. 2C**). Based on these results, we hypothesized that additional intracellular signals may trigger ECM detachment-induced autophagy in MECs independently of the PI3K-AKT-MTORC1 pathway.

IKK activation promotes autophagy induction upon substratum detachment in epithelial cells. Recently, the Kroemer group has reported that activation of the IKK complex contributes to induction of autophagy in response to diverse stimuli.[8] We therefore investigated whether IKK is activated in response to ECM detachment in MECs. MCF10A cells were grown attached or in suspension for 24 h; thereafter, the endogenous IKK complex was immunoprecipitated from protein lysates and its activation status was evaluated by immunobloting. As shown in **Figure 3A**, matrix detachment induced phosphorylation of the activation sites of IKK [CHUK(Ser176,180)/IKBKB(Ser177,181)]. Moreover, potent phosphorylation on the IKK substrate, NFKBIA/IκBα was also detected in suspended, but not in attached cells. Together, these data support that the IKK complex is activated during ECM detachment in MCF10A cells. Notably, activation of the IKK complex was not observed in MEFs lacking ECM contact (**Fig. S2**), indicating that this signaling pathway was distinctly activated in MECs in response to ECM detachment.

Next, we investigated whether inhibition of IKK was sufficient to prevent autophagy induction during ECM detachment. MCF10A cells were cultured in attached or suspended conditions for 24 h in the presence or absence of the IKK kinase inhibitor Bay-117082.[21] A significant reduction in autophagic flux was observed in suspended cells treated with Bay-117082 (**Fig. 3B**). In addition, in MCF-10A cells stably expressing GFP-LC3, Bay-117082 potently suppressed GFP-LC3 puncta formation during ECM detachment (**Fig. 3C**). Furthermore, Bay-117082 treatment efficiently suppressed NFKBIA phosphorylation, but did not significantly alter the activation status of AKT or MTORC1 in suspended cells (**Fig. 3D**). We corroborated these results using loss-of-function approaches targeting various IKK complex components. First, we utilized MCF10A cells expressing dominant negative CHUK (DN-CHUK)[22] or IKBKB (DN-IKBKB)[23] to inhibit IKK activation in detached cells. Compared with controls, the expression of DN-IKBKB suppressed LC3-II conversion and turnover in ECM detached cells (**Fig. 4A**), whereas DN-CHUK had minimal effects on autophagy induction. Consistent with this observation, DN-IKBKB, but not DN-CHUK, suppressed NFKBIA phosphorylation in suspended cells (**Fig. 4B**). Neither DN-CHUK nor DN-IKBKB significantly affected MTORC1 activity in suspended cells, as evidenced by RPS6 phosphorylation. Furthermore, RNAi-mediated depletion of the key regulatory component of the IKK complex, IKBKG, also potently inhibited LC3-II conversion and turnover during ECM detachment (**Fig. 4C**). Once again, upon IKBKG depletion, phosphorylation of NFKBIA was decreased in suspended cells, but no significant changes were observed in the phosphorylation status of AKT and RPS6 in IKBKG knockdown cells compared with controls.

Multiple signaling pathways regulate IKK complex activation[24] and one of these upstream regulators, MAP3K7/TAK1, has been linked to autophagy induction.[8] Accordingly, RNAi-mediated depletion of MAP3K7 significantly suppressed NFKBIA phosphorylation during ECM detachment as well as attenuated detachment-induced autophagy, without impacting AKT or MTORC1 activity in suspended cells (**Fig. 4D**). Taken together, these data indicate that, in contrast to mouse fibroblasts, the MAP3K7-IKK axis plays a critical role in ECM detachment-induced autophagy in MECs.

Because recent work suggests that IKK complex activation promotes autophagy via an NFKB-independent mechanism, we further assessed whether NFKB activation was specifically required for detachment-induced autophagy. MCF10A cells were stably infected with a retroviral construct expressing IκB superrepressor (IκB-SR), a mutant form of NFKBIA^{S32A,S36A} that does not undergo signal-induced phosphorylation and degradation. Expression of IκB-SR efficiently blocks NFKB nuclear translocation and prevents target gene transcription.[25] As shown in **Figure S3**, overexpression of IκB-SR effectively blocked the phosphorylation of NFKBIA in response to ECM deprivation or TNF/TNFα treatment. However, no significant change on LC3-II conversion and turnover was observed between suspended cells expressing control vector or IκB-SR. Overall, this data indicates that autophagy in ECM deprived mammary epithelial cells is induced in an IKK-dependent, NFKB-independent manner.

Antibody-mediated function blockade of ITGA3-ITGB1 induces IKK activation and autophagy in MECs. Integrins are the major receptors for cell adhesion to the ECM that transduce outside-in signals from the ECM.[26] Hence, we tested whether autophagy induction during ECM detachment directly results from the blockade of signals emanating from specific

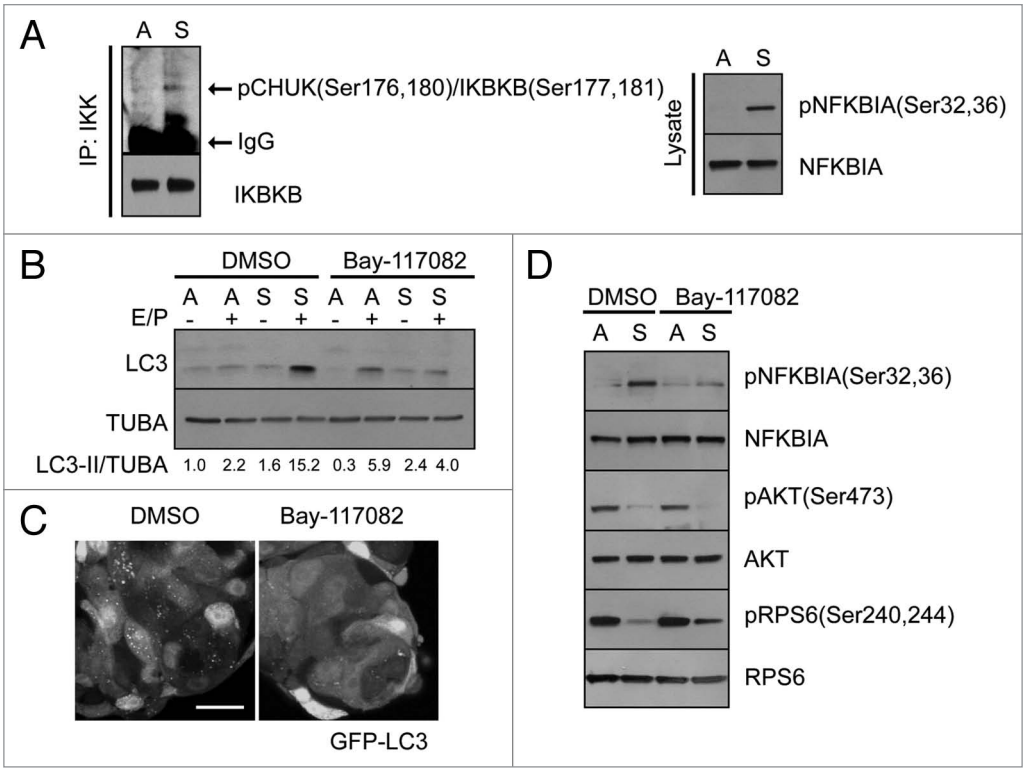

Figure 3. Inhibition of IKK activity suppresses autophagy induction in ECM deprived MECs. (**A**) Left: Lysates from MCF10A cells grown in attached (A) or suspended (S) for 24 h were subject to immunoprecipitation with antibodies against CHUK and IKBKB. Immunoprecipitates were subject to immunoblotting with antibodies against phospho-CHUK(Ser176,180)/IKBKB(Ser177,181). Right: Lysates from MCF10A cells grown in attached (A) or suspended (S) for 24 h were subject to immunoblotting with antibodies against phospho-NFKBIA(Ser32,36) [pIkBa(Ser32,36)] and NFKBIA (IκBα). (**B**) MCF10A cells treated with DMSO or 10 μM Bay-117082 were grown attached (A) or suspended (S) for 24 h, lysed and immunoblotted with anti-LC3 and anti-TUBA antibodies. Where indicated, E64d and pepstain A (E/P) were added 6 h prior to harvesting. (**C**) MCF10A cells stably expressing GFP-LC3 were grown suspended for 24 h in the presence of DMSO (left) or 10 μM Bay-117082 (right). Scale bar: 25 μm. (**D**) MCF10A cells treated with DMSO or 10 μM Bay-117082 were grown attached (A) or suspended (S) for 24 h, lysed and immunoblotted with the indicated antibodies.

integrin subunits. Extending our previous results,[4] incubation of MCF10A cells with ITGB1 function-blocking antibody AIIB2 caused severe cell detachment and rounding (**Fig. 5A**, left), as well as increased LC3-II conversion and turnover (**Fig. 5A**, right). Moreover, we also observed a significant elevation of NFKBIA phosphorylation in AIIB2 treated cells (**Fig. 5B**), indicating that blockade of ITGB1 function resulted in activation of the IKK pathway. The integrin complexes ITGA3-ITGB1 and ITGA6-ITGB4 (α6β4 integrin) are the major receptors for LAMA5 (laminin-5), an important component of the epithelial cell basement membrane.[27,28] To further ascertain how each of these integrin receptor subunits contributes to IKK activation and autophagy induction during ECM detachment, we preincubated cells with function-blocking antibodies directed against each integrin subunit. As shown in **Figure 5C**, MCF10A cells stably expressing GFP-LC3 were preincubated with function-blocking antibodies against ITGA3 (P1B5),[29] ITGB1 (AIIB2),[30] ITGA6 (G0H3),[31] or ITGB4 (ASC-8)[32] for 30 min and seeded onto tissue culture plates coated with laminin-rich reconstituted basement membrane (rBM). After 16 h, IgG treated control cells were fully adherent to culture plates. Cells incubated with function-blocking antibodies against the ITGA3, ITGA6 or ITGB4 integrin subunits were also attached and spread on the plates, whereas anti-ITGB1 antibody-treated cells failed to spread on this substratum and remained only partially attached to the plate (**Fig. 5C**). ITGB1 function blockade induced potent GFP-LC3 puncta formation in MCF10A cells. Moreover, we also observed strong induction of GFP-LC3 puncta in response to the block in ITGA3 functions. In contrast, no increase in punctate GFP-LC3 was present in IgG-treated controls or in cells incubated with anti-ITGA6 or ITGB4 antibodies (**Fig. 5C**). Together, these results suggest that a block in the function of the ITGA3-ITGB1 complex is sufficient to induce autophagy. Moreover, the blockade of either ITGA3 or ITGB1 caused an increase in NFKBIA phosphorylation, while blockade of ITGA6 or ITGB4 had less pronounced effects (**Fig. 5D**). These results motivated the hypothesis that the specific loss in ITGA3-ITGB1 function stimulates autophagy via activation of the IKK pathway.

To further test this prediction, we evaluated whether IKK pathway inhibition is sufficient to prevent autophagosome (GFP-LC3 puncta) induction during ITGA3-ITGB1 blockade. Because anti-ITGB1 antibody treatment causes severe cell rounding, the rigorous quantification of GFP-LC3 was not technically possible; as a result, we employed anti-ITGA3 for these experiments. MCF10A cells stably expressing GFP-LC3 were

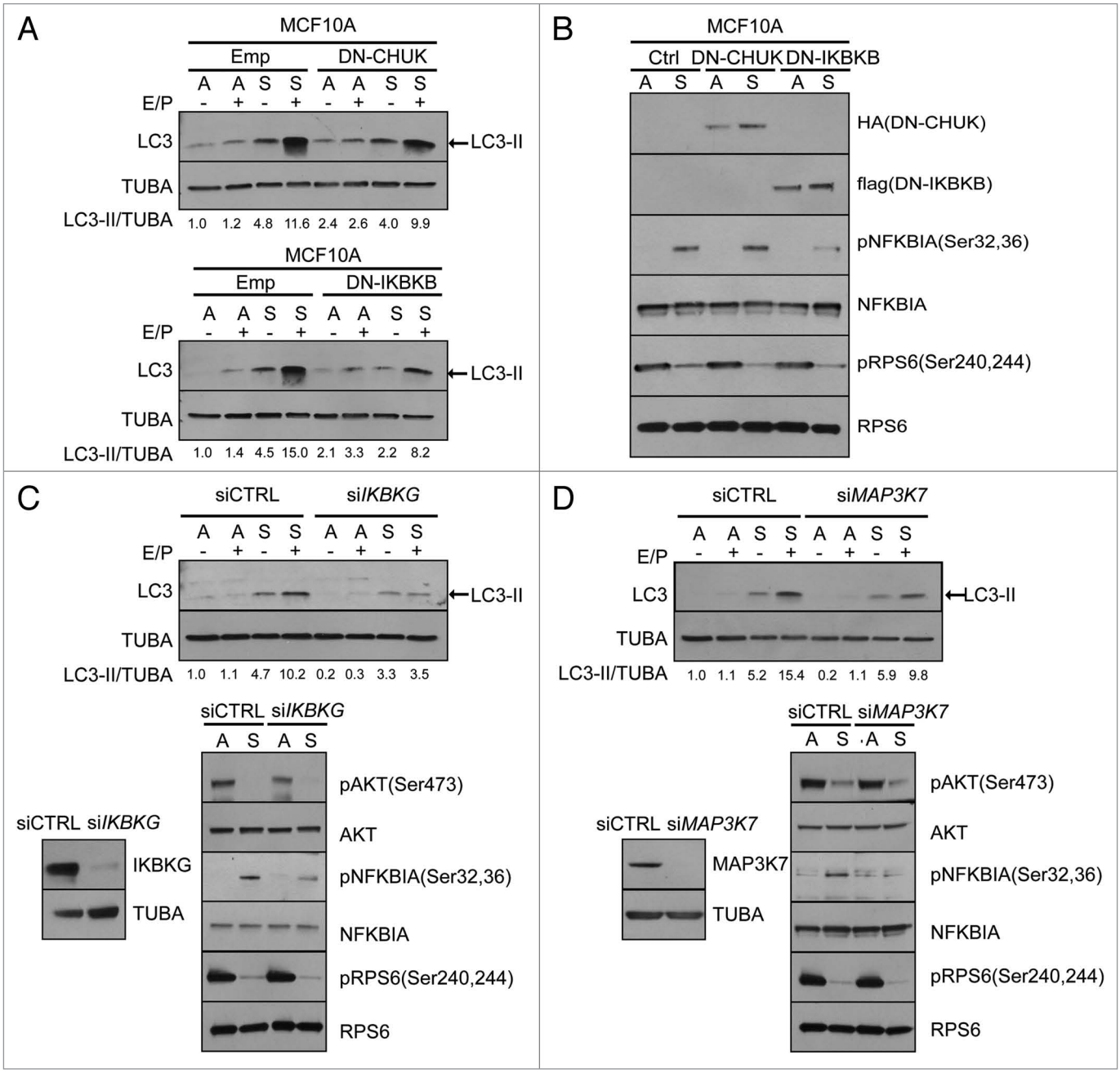

Figure 4. MAP3K7/IKK pathway promotes ECM detachment-induced autophagy in MECs. (**A**) MCF10A cells transiently transected with empty vector (Emp), vector expressing dominant negative CHUK (DN-CHUK) (top), or dominant negative IKBKB (DN-IKBKB) (bottom) were grown attached (A) or suspended (S) for 24 h, lysed and immunoblotted with anti-LC3 and anti-TUBA antibodies. Where indicated, E64d and pepstain A (E/P) were added 6 h prior to harvesting. LC3-I detection was minimal in this experiment. (**B**) MCF10A cells transiently transected with empty vector (Emp), vector expressing DN-CHUK or DN-IKBKB were grown attached (A) or suspended (S) for 24 h, lysed and immunoblotted with the indicated antibodies. (**C**) Top: MCF10A cells transfected with siCTRL or si*IKBKG* were grown attached or suspended for 24 h. Where indicated, E64d and pepstain A (E/P) were added 6 h prior to harvesting. Cell lysates were subject to immunoblotting with antibodies against LC3 and TUBA. LC3-I detection was minimal in this experiment. Bottom left: IKBKG protein levels in MCF10A cells transfected with siCTRL or si*IKBKG*. Bottom right: siCTRL or si*IKBKG* expressing MECs were grown attached or suspended for 24 h, lysed and immunoblotted with indicated antibodies. (**D**) Top: MCF10A cells transfected with siCTRL or si*MAP3K7* were grown attached or suspended for 24 h. Where indicated, E64d and pepstain A (E/P) were added 6 h prior to harvesting. Cell lysates were subject to immunoblotting with antibodies against LC3 and TUBA. LC3-I detection was minimal in this experiment. Bottom left: MAP3K7 protein levels in MCF10A cells transfected with siCTRL or si*MAP3K7*. siCTRL or si*MAP3K7*-expressing MECs were grown attached or suspended for 24 h, lysed and immunoblotted with the indicated antibodies.

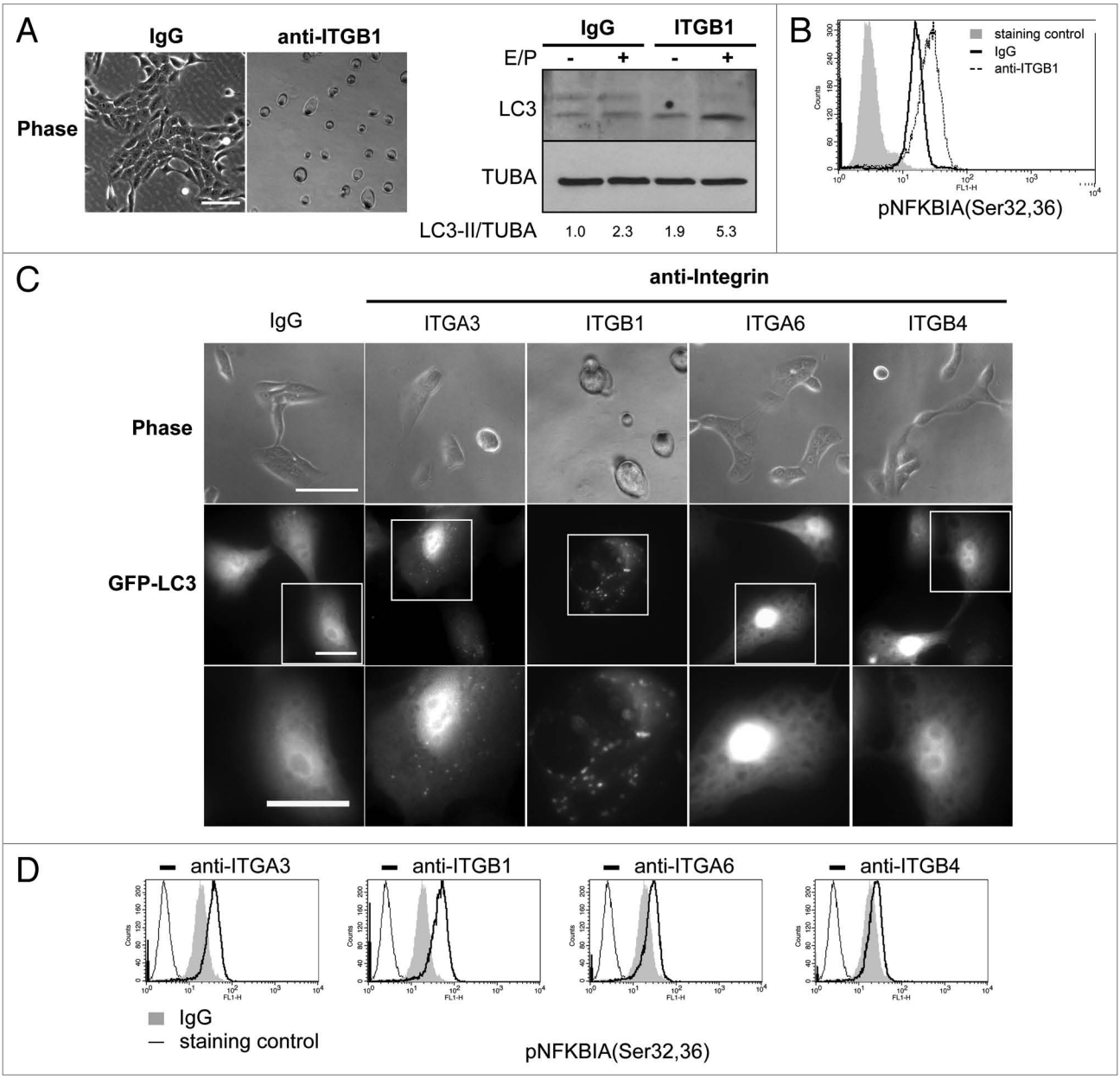

Figure 5. Antibody-mediated blockade of ITGA3-ITGB1 function induces IKK activation and autophagy in MECs. (**A**) Left: Phase images of MCF10A cells incubated with 20 μg/ml IgG or anti-ITGB1 prior to seeding to rBM (Matrigel)-coated culture plates for 24 h. Scale bar: 100 μm. Right: MCF10A cells pre-incubated with 20 μg/ml IgG or anti-ITGB1 were cultured on rBM-coated culture plates for 24 h. Cell lysates were subject to immunoblotting against LC3 and TUBA. Where indicated, E64d and pepstain A (E/P) were added 6 h prior to harvesting. (**B**) MCF10A cells were preincubated with 20 μg/ml IgG or anti-ITGB1 prior to seeding to rBM-coated culture plates for 24 h. pNFKBIA(Ser32,36) levels were detected by flow cytometry in permeabilized cells. (**C**) MCF10A cells expressing GFP-LC3 were incubated with the indicated antibodies at 20 μg/ml before seeding to rBM-coated culture plates for 16 h. Top: Phase images. Scale bar: 100 μm. Middle: Fluorescent images of GFP-LC3. Scale bar: 20 μm. Bottom: enlarged images of indicated area in middle panel. Scale bar: 40 μm. (**D**) Flow cytometry detection of intracellular levels of pNFKBIA(Ser 32,36) in cells preincubated with the indicated antibodies before seeding to rBM-coated culture plates for 16 h.

transfected with si*IKBKG* and si*MAP3K7* to target the IKK pathway as well as with si*TSC2* to target the MTORC1 pathway. Moreover, nontargeting siRNA (siCTRL) and siRNA against the key autophagy regulator, *ATG7* (si*ATG7*) were used as negative and positive controls, respectively. Cells were preincubated with anti-ITGA3 antibody and seeded onto laminin-rich rBM coated plates. After 16 h, the number of GFP-LC3 puncta per cell was enumerated (**Fig. 6**). Cells expressing control siRNA exhibited numerous GFP-LC3 puncta in response to the block in ITGA3 function, which was potently suppressed upon ATG7 depletion. Moreover, the knockdown of IKBKG and MAP3K7 significantly decreased GFP-LC3 puncta formation in response to ITGA3 function blocking antibody; in contrast, TSC2 depletion had minimal effects on GFP-LC3 puncta formation compared with

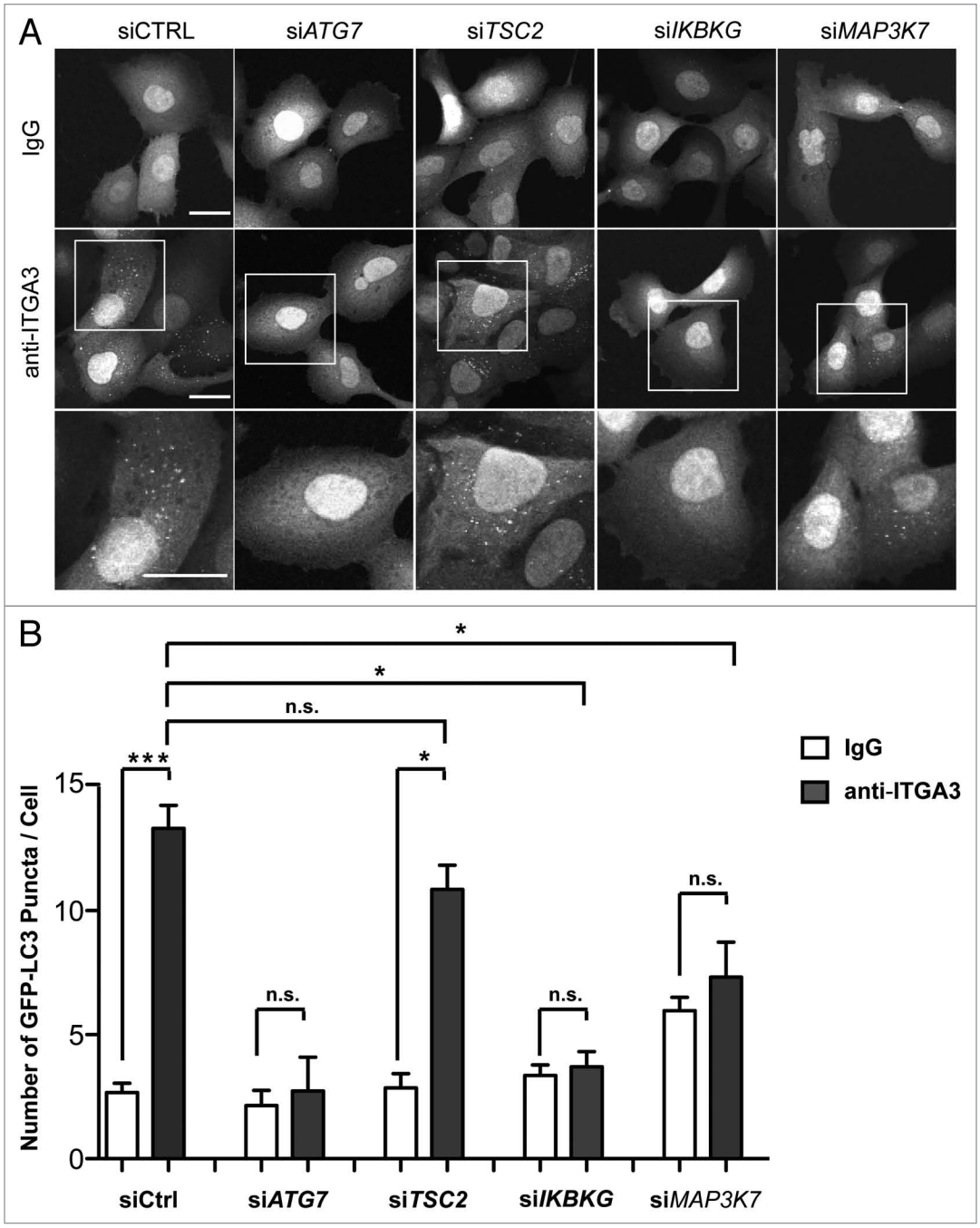

Figure 6. MAP3K7-IKK pathway promotes autophagy in MECs induced upon function blockade of ITGA3. (**A**) Confocal images of MCF10A cells expressing GFP-LC3 transfected with the indicated siRNAs, preincubated with IgG (top) or anti-ITGA3 antibody (middle), and seeded to rBM-coated culture plates for 16 h. Scale bar: 25 μm. Bottom: Enlarged images of the indicated area in middle panel. Scale bar: 50 μm. (**B**) Quantification of number of GFP-LC3 puncta per cell (mean ± SEM). In total, 300 cells from three independent experiments were quantified.

cells expressing control siRNA. Together, these data indicated that the disruption of ITGA3-ITGB1 function causes IKK activation and autophagosome induction in MCF10A cells.

Pharmacological Inhibition of IKK activity enhances luminal apoptosis of MCF10A cells in 3D culture. Autophagy promotes cell survival during ECM detachment.[4] Hence, we investigated whether IKK inhibition would enhance cell death in cells devoid of interaction with the ECM. MCF10A cells were treated with varying doses of IKK inhibitor Bay-117082 and cultured in attached vs. detached conditions for 24 h, upon which apoptosis was monitored by immunoblotting for cleaved-PARP. As shown in **Figure 7A**, cleaved-PARP was only detected in detached cells, indicating ECM detachment induced anoikis in these cells. Interestingly, Bay-117082 treatment enhanced cleaved-PARP expression in a dose-dependent manner, confirming that IKK pathway inhibition enhanced apoptosis in suspended cells.

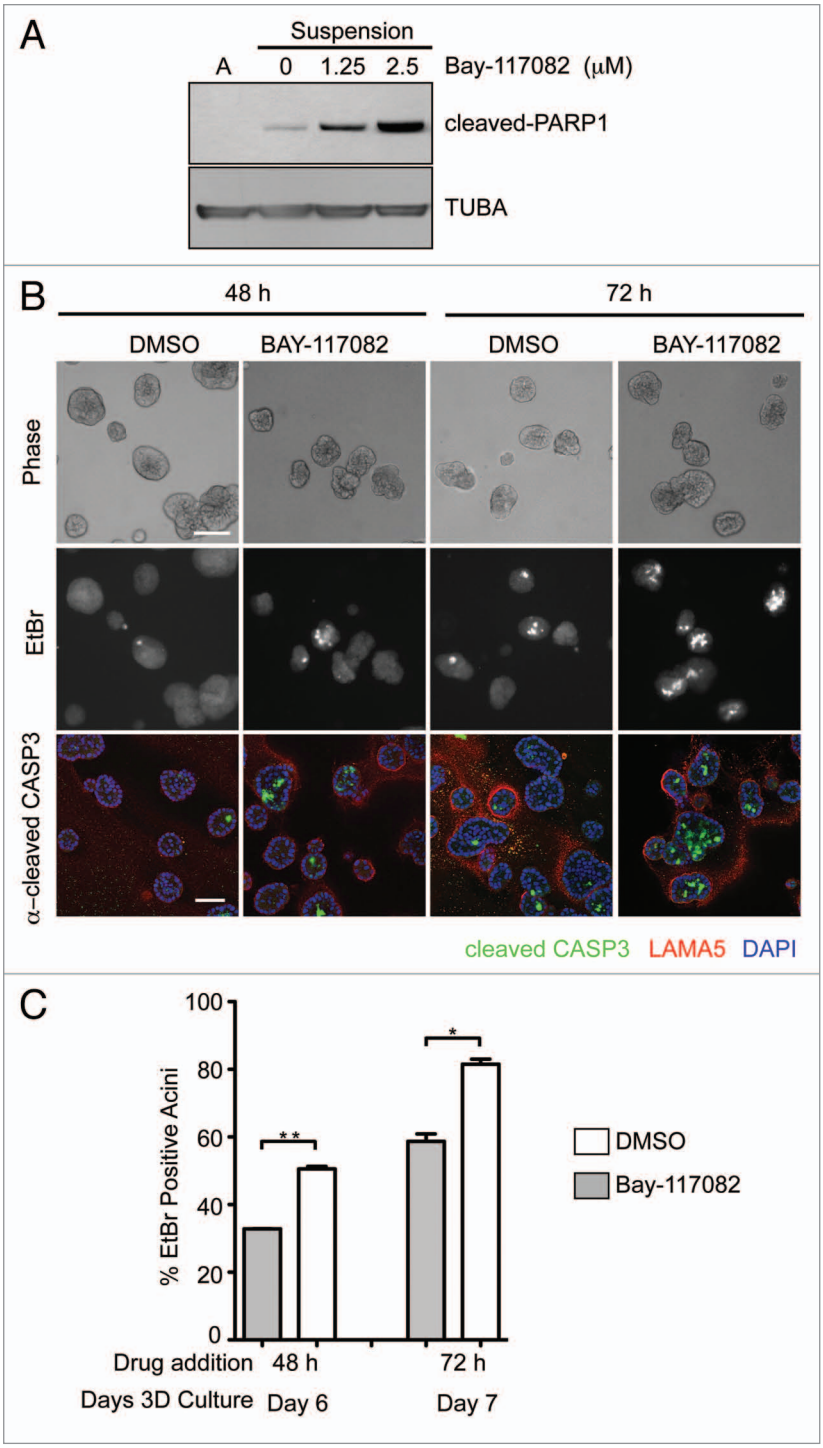

Figure 7. Inhibition of IKK enhances anoikis and luminal apoptosis in 3D culture. (**A**) MCF10A cells were cultured attached (A) or in suspension in the presence of DMSO control or Bay-117082 at the indicated doses. Cell lysates were subject to immunoblotting with indicated antibodies. (**B**) Top: Phase images of MCF10A cell in 3D culture treated with DMSO or 10 μM Bay-117082 for indicated period of time. Scale bar: 100 μm. Middle: Fluorescent images of EtBr staining of MCF10A cell 3D culture under indicated conditions. Bottom: Confocal images of cleaved-CASP3 staining of MCF10A cell 3D culture treated with indicated conditions. Scale bar: 50 μm. (**C**) Quantification of percentage of EtBr positive acini in MCF10A 3D culture under the indicated conditions (mean ± SEM). In total, 300 acini from three independent experiments were quantified.

To further corroborate the effects of IKK inhibition on anoikis, we utilized a three-dimensional (3D) culture model in which MCF10A cells form spherical acini notable for a hollow lumen. In this model, the anoikis of cells deprived of ECM contact is a principal contributor to the selective cell death of centrally located cells during lumen formation.[33] MCF10A cells were grown in 3D culture for 4 d, a time point at which minimal luminal apoptosis is observed.[34] Thereafter, the cultures were acutely treated with Bay-117082, and cell death was monitored on subsequent days by staining with ethidium bromide (EtBr), a DNA-binding intravital dye incorporated into dying cells.[34] We observed increased EtBr staining within the centers of acini treated with Bay-117082 at both 48 h and 72 h. This correlated with increased cleaved-CASP3/caspase3 staining of cells occupying the luminal space following treatment with Bay-117082 (**Fig. 7B**). Quantification of the percentage of EtBr positive acini in control and Bay-117082 treated structures revealed that Bay-117082 significantly accelerated luminal cell death in 3D culture (**Fig. 7C**). Overall, these results corroborate that pharmacological IKK inhibition enhances anoikis and accelerates luminal apoptosis during MCF10A acinar morphogenesis in three-dimensional culture.

Discussion

Here, we demonstrated that ECM detachment induces autophagy in mouse fibroblasts and human mammary epithelial cells through distinct pathways. In MEFs, the reduced activation of PI3K-AKT-MTORC1 pathway is the principal mediator of ECM detachment-induced autophagy; as a result, sustained activation of the PI3K-AKT-MTORC1 pathway is sufficient to suppress autophagy in ECM deprived MEFs. On the other hand, the MAP3K7-IKK pathway is the major contributor to autophagy induction in MECs during ECM detachment. In addition, we uncover that the specific loss of ITGA3-ITGB1 function in MECs is sufficient to induce autophagy via IKK activation, thus linking the deactivation of integrin receptors to specific intracellular signals that direct autophagy induction. Furthermore, pharmacological inhibition of IKK enhances anoikis and accelerates luminal cell apoptosis in 3D cultures of MCF10A cells.

The importance of the PI3K-AKT-MTORC1 pathway in autophagy regulation is well established.[35] Various stimuli that inhibit PI3K-AKT-MTORC1 pathway also activate autophagy. Moreover, activation of the PI3K-AKT-MTORC1 pathway has also been associated with autophagy inhibition. An increase of class I PI3K products

(phosphatidylinositol 3,4-bisphosphate and phosphatidylinositol 3,4,5-triphosphate) reduces autophagy in HT-29 cells.[36] AKT activation also suppresses autophagy in apoptosis-deficient tumor cells.[37] Here, we demonstrated that activation of the PI3K-AKT-MTORC1 pathway is similarly sufficient to suppress detachment-induced autophagy in fibroblasts. In contrast, activation of the MAPK1/3 (ERK2/1 respectively) pathway does not potently suppress autophagy during ECM detachment (data not shown and ref. 38), indicating a unique role for the PI3K-AKT pathway in autophagy regulation in ECM-detached fibroblasts.

Importantly, we demonstrated a new functional requirement for the IKK complex in the stimulating detachment-induced autophagy in mammary epithelial cells (MECs). Recent work indicates that IKK activation induces autophagy in response to multiple known autophagy stimuli.[8] We showed that inhibition of IKK activity can suppress autophagy even when MTORC1 pathway activation is profoundly suppressed; based on this result, we construe that the IKK complex plays a direct and critical role in autophagy regulation in detached MECs. Consistent with previous studies,[8,11] suppressing NFKB activity is not sufficient to prevent autophagy induction in suspended cells (**Fig. S3**), indicating that the IKK complex regulates detachment-induced autophagy via a NFKB independent pathway. Remarkably, the depletion of IKBKB and IKBKG, but not CHUK, significantly suppresses autophagy induction during ECM detachment. Although CHUK and IKBKB are closely related, these kinases target distinct substrates and have divergent biological roles.[10] For example, CHUK and IKBKB are differentially involved in cytokine- and insulin-induced MTORC1 activation.[39] Our work suggests that IKBKB has a more direct role in regulating autophagy in the context of ECM detachment. Notably, the IKK phosphorylation consensus DSΨXXS[40] is present in several autophagy molecules, including ULK2, RB1CC1/FIP200, ATG14 and KIAA0226/Rubicon. Hence, IKK complex may directly impact certain initiation steps during autophagosome induction. Alternatively, IKK activation may induce phosphorylation and degradation of negative regulators of autophagy, resulting in autophagy activation. The further scrutiny of the precise mechanisms through which IKK activation leads to autophagy induction in ECM detached cells remains an important topic for future study.

Notably, although our results reveal striking differences in the pathways regulating ECM detachment-induced autophagy in MEFs and MCF10A cells, we recognize that the distinct results observed in these two cell types may represent unique situations in which detachment-induced autophagy is principally triggered by a single pathway. Accordingly, we hypothesize that in most cells, including other epithelial cell types, the induction of autophagy during ECM-deprivation likely involves the integration of multiple signaling pathways, which potentially includes downregulation of MTORC1 activity, stimulation of the IKK complex, as well as other pathways that presently remain undefined. Indeed, two important areas for further study include: (1) elaborating the larger repertoire of signals controlling detachment-induced autophagy, both MTORC1-dependent and -independent; and (2) dissecting how these multiple signals are integrated to produce the overall autophagic response in ECM-deprived cells.

Moreover, we uncovered a new link between integrin receptor signaling and autophagy induction. The ITGA3-ITGB1 and ITGA6-ITGB4 integrin receptors have overlapping ligand-binding specificities, and both have been reported to have prosurvival functions in keratinocytes and epithelial cells.[41] Based on antibody-mediated function blocking experiments, our studies point to the loss of ITGA3-ITGB1 receptor engagement as the specific trigger for autophagy induction. Furthermore, this blockade also causes a significant increase in NFKBIA phosphorylation, and RNAi-mediated depletion of IKBKG and MAP3K7 significantly inhibits autophagosome formation in response to the block in ITGA3 function. Altogether, these results support a model in which reduced ITGA3-ITGB1 function in detached cells stimulates autophagy via activation of the MAP3K7-IKK pathway.

Both the NFKB pathway and autophagy have been found to promote cell survival during ECM detachment.[4,7] Our study demonstrates that pharmacological inhibition of IKK enhances anoikis and accelerates luminal cell apoptosis in 3D culture of mammary epithelial cells; we propose that increased cell death results from simultaneous suppression of NFKB targets and autophagy upon inhibition of the IKK complex, thereby increasing cell susceptibility to anoikis. Remarkably, the prosurvival functions of NFKB pathway and autophagy have both been implicated in the adhesion-independent growth and anoikis resistance of tumor cells.[38,42-45] Because anoikis resistance is associated with cancer progression and metastasis, in future work, it will be important to further scrutinize whether IKK critically regulates detachment-induced autophagy in cancer cells as well as to ascertain if IKK inhibition can be exploited to inhibit cancer cell survival in foreign tissue environments.

Materials and Methods

Cell culture. *Tsc2*$^{+/+}$ and *tsc2*$^{-/-}$ MEFs were generously provided by Dr. David Kwiatkowski (Harvard Medical School) and cultured in DMEM containing 25 mM glucose (Invitrogen, 11965118) supplemented with 10% fetal bovine serum (Atlas Biologicals, FP-0500-A), penicillin and streptomycin (UCSF Cell Culture Facility, CCFGK004). MCF10A cells were cultured as described previously.[34] Stable cell lines were generated by selection with 2 μg/ml Puromycin (Sigma, P7255) or 300 μg/ml G418 (Sigma, A1720).

Antibodies and chemicals. The anti-LC3 antibody generated in our laboratory has been described previously and is now commercially available (EMD Millipore, ABC232).[4] The following antibodies were purchased from Cell Signaling Technology: anti-TSC2 (3612), anti-phospho RPS6 ribosomal protein (Ser240/244) (2215), anti-RPS6 ribosomal protein (2217), anti-phospho-RPS6KB1/p70RPS6 Kinase (Thr389)(9234), anti-RPS6KB1/p70RPS6 Kinase (9202), anti-phospho-AKT(Ser473) (4058), anti-AKT (4685), anti-phospho-CHUK/IKKα(Ser176) and IKBKB/IKKβ(Ser177) (2078), anti-IKBKG/IKKγ (2678), anti-phospho-NFKBIA/IκBα(Ser32/36) (9246), anti-NFKBIA/IκBα (4814), anti-cleaved-PARP (9532), anti-cleaved CASP3/Caspase 3 (9579). Other antibodies used include following: anti-TUBA/tubulin (Sigma, T6199), anti-HA (HA.11 Clone 16B12,

Covance, MMS-101R), anti-Flag (Sigma, F3165), anti-ITGB1/integrin β1 (Developmental Studies Hybridoma Bank, AIIB2), anti-ITGA3/integrin α3 (P1B5, EMD Millipore, MAB1952), anti-ITGA6/integrin α6 (G0H3, EMD Millipore, MAB1378), anti-ITGB4/Integrin β4 (ASC8, EMD Millipore, MAB2059), anti-phospho-NFKBIA/IκBα(Ser32/36) (Abcam, ab12135), anti-CHUK and IKBKB (IKKα/β) (Santa Cruz Biotechnology, sc-7607), anti-laminin5 (EMD Millipore, MAB19562). Chemicals used include: poly(2-hydroxyethyl methacrylate) (poly-HEMA) (Sigma, P3932), E64d (Sigma, E8640), pepstatin A (Sigma, P4265), Bay-117082 (Sigma, B5556).

DNA constructs. pcDNA *TSC2* was a generous gift from Dr. Brendan Manning (Harvard School of Public Health) and pBABE-*IκB-SR* was a generous gift from Dr. Joan Brugge (Harvard Medical School). The following constructs were obtained from Addgene: pcDNA-*CHUK*^{K44M}/*IKKα*^{K44M}-HA (plasmid 23297), pCR-Flag-*IKBKB*^{K44M}/IKKβ^{K44M} (plasmid 15466), pcDNA3-*FLAG-RHEB* (plasmid 19996).

Retroviral production. pWZLneo ER-AKT and pBABEpuro GFP-LC3 have been previously described.[4,46] The retroviral vector pLNCX-neo containing active PIK3CA* (*PIK3CA*^{E545K}) was kindly provided by Dr. W. Weiss (University of California, San Francisco). *RHEB* was cloned into pMX-puro retroviral vector. *TSC2* WT and *TSC2*^{N1643I} were cloned into pBABE-puro retroviral vector. Retrovirus was generated using as previously described.[34]

RNA interference. The following pooled small interfering RNA (siRNA) oligonucleotides (SMARTpool) against *TSC2* (L-003029-00-0005), *ATG7* (M-020112-01-0005), *IKBKG* (L-003767-00-0005) and *MAP3K7* (L-003790-00-0005) were purchased from Dharmacon RNA Technologies. For siRNA transfection, 2 × 10^6 MCF10A cells were transfected with 200 nM siRNA using Amaxa nucleofector kit V (Lonza, VCA-1003). After 36 to 48 h, cells were utilized for substratum detachment assays or antibody-mediated blockade of integrin subunit function.[4]

Substratum detachment assays. MCF10A cells were cultured attached or suspended as previously described.[4,47] Briefly, tissue culture plates coated with 6 mg/ml poly-HEMA in 95% ethanol were incubated at 37°C until dry. Cells were subsequently plated on poly-HEMA–coated plates in their appropriate growth medium. To detect cleaved-PARP during anoikis, MCF10A cells were cultured in suspension for indicated times in DMEM/F12 media containing 0.5% horse serum (Invitrogen, 16050-114), 0.5 μg/ml hydrocortisone (Sigma, H0888), 100 ng/ml cholera toxin (Sigma, C8052), penicillin and streptomycin.

To evaluate autophagic flux, the lysosomal inhibitors, E64d and pepstatin A (E/P), were added directly to the culture media at 10 μg/ml at 6 h before lysis. Lysates were resolved by SDS-PAGE, subject to anti-MAP1LC3A and anti-TUBA immunoblotting, and the levels of cleaved and PE-lipidated LC3-II and TUBA were quantified using densitometry. The change in the LC3-II/TUBA ratio in the presence of E/P between detached and suspended conditions was used to assess autophagic flux; in addition, the levels of LC3-II/TUBA during suspension in the presence of E/P (lanes corresponding S + E/P) were directly compared with assess the overall capacity for autophagy induction upon detachment.

Immunoprecipitation. MCF10A cells grown attached or suspended for 24 h were lysed in Triton lysis buffer (0.5% Triton (v/v), 150 mM NaCl, 20 mM Tris pH 7.5, 2 mM EDTA pH 8.0) containing protease inhibitors cocktail (Sigma, P8340), 10 mM NaF (Sigma, S6776), 10 mM β-glycerophosphate (Sigma, G9422) 1 mM Na_3VO_3 (Sigma, S6508) and 10 nM calyculin A (Sigma, C5552). Lysates were homogenized with a Dounce homogenizer (Fisher Scientific, K885300-0002) and incubated on ice for 30 min. Subsequently, the lysates were cleared by centrifuge for 20 min at 4°C. 1 mg of each cell lysate was precleared with protein A/G agarose (Santa Cruz, sc-2003) at 4°C for 1 h and incubated with 10 μg/ml of anti-CHUK and IKBKB (IKKα/β) antibody overnight at 4°C. Subsequently, protein A/G agarose was added to lysate and incubated for 2 h at 4°C; the immune complex-containing agarose beads were recovered by centrifugation, washed 3 times with cold lysis buffer containing protease and phosphatase inhibitors, and subject to SDS-PAGE and immunoblot analysis.

Flow cytometry. Cells were harvested and fixed in 4% paraformaldehyde followed by resuspension in cold 90% methanol for 30 min on ice. Cells were then subject to antibody staining according to manufacturer's protocol. Anti-phospho-NFKBIA/IκBα(Ser32/36) (Abcam, ab12135) was used at 1:100 dilution.

Antibody-mediated blockade of integrin subunit function. Tissue culture plates or coverslips were coated with 1% laminin rich reconstituted basement membrane (v/v) (Matrigel, BD Bioscience, 354234) in PBS at 37°C for 16 h. MCF10A cells were trypsinized and resuspended in 100 μl full growth media at 1 × 10^6/ml. The indicated anti-integrin subunit antibodies or isotype controls were added to cell suspension at final concentration of 20 μg/ml. Cells were incubated on ice for 30 min, diluted with full culture media and seeded to rBM (Matrigel)-coated tissue culture plates or coverslips. After 16 to 24 h, cells were harvested for experiments.

Three-dimensional culture assays. MCF10A 3D cultures were performed and processed for ethidium bromide (EtBr) staining or confocal microscopy as described previously.[34] When indicated, 10 μM Bay-117082 was added to 3D cultures on day 4 for 48 and 72 h before fixation.

Image acquisition and analysis. Phase images of 3D culture were acquired on an Axiovert 200 microscope (Carl Zeiss Microscopy) equipped with a Spot RT camera (Diagnostic Instruments). For confocal analyses, images were acquired using a C1Si confocal laser-scanning microscope (Nikon) and analyzed using EZ-C1 software (v3.20) (Nikon) and MetaMorph software (v6.0) (MetaMorph software, GE Healthcare). 3D cultures were fixed and stained as previously described.[34]

Statistical analysis. Graphs represent the average values from three independent experiments with error bars reflecting the standard error of the mean. GraphPad Prism software (v5.0b) (GraphPad Software) was used for statistical analysis. p values were determined by unpaired Student's t-test with $p < 0.05$ considered significant.

Disclosure of Potential Conflicts of Interest

No potential conflicts of interest were disclosed.

Acknowledgments

We thank Drs. Joan Brugge, David Kwiatkowski, Brendan Manning and William Weiss for reagents and other members of the Debnath laboratory for helpful discussions. Grant support to J.D. includes the NIH (RO1 CA126792 and ARRA supplement CA126792-S1) and the DOD BCRP (W81XWH-11-1-0130).

Supplemental Materials

Supplemental materials may be found here:
www.landesbioscience.com/journals/autophagy/article/24870

References

1. Gilmore AP. Anoikis. Cell Death Differ 2005; 12(Suppl 2):1473-7; PMID:16247493; http://dx.doi.org/10.1038/sj.cdd.4401723
2. Frisch SM, Francis H. Disruption of epithelial cell-matrix interactions induces apoptosis. J Cell Biol 1994; 124:619-26; PMID:8106557; http://dx.doi.org/10.1083/jcb.124.4.619
3. Debnath J, Brugge JS. Modelling glandular epithelial cancers in three-dimensional cultures. Nat Rev Cancer 2005; 5:675-88; PMID:16148884; http://dx.doi.org/10.1038/nrc1695
4. Fung C, Lock R, Gao S, Salas E, Debnath J. Induction of autophagy during extracellular matrix detachment promotes cell survival. Mol Biol Cell 2008; 19:797-806; PMID:18094039; http://dx.doi.org/10.1091/mbc.E07-10-1092
5. He C, Klionsky DJ. Regulation mechanisms and signaling pathways of autophagy. Annu Rev Genet 2009; 43:67-93; PMID:19653858; http://dx.doi.org/10.1146/annurev-genet-102808-114910
6. Avivar-Valderas A, Bobrovnikova-Marjon E, Alan Diehl J, Bardeesy N, Debnath J, Aguirre-Ghiso JA. Regulation of autophagy during ECM detachment is linked to a selective inhibition of mTORC1 by PERK. Oncogene 2012; PMID:23160380; http://dx.doi.org/10.1038/onc.2012.512
7. Yan SR, Joseph RR, Rosen K, Reginato MJ, Jackson A, Allaire N, et al. Activation of NF-kappaB following detachment delays apoptosis in intestinal epithelial cells. Oncogene 2005; 24:6482-91; PMID:16007176
8. Criollo A, Senovilla L, Authier H, Maiuri MC, Morselli E, Vitale I, et al. The IKK complex contributes to the induction of autophagy. EMBO J 2010; 29:619-31; PMID:19959994; http://dx.doi.org/10.1038/emboj.2009.364
9. Siebenlist U, Franzoso G, Brown K. Structure, regulation and function of NF-kappa B. Annu Rev Cell Biol 1994; 10:405-55; PMID:7888182; http://dx.doi.org/10.1146/annurev.cb.10.110194.002201
10. Chariot A. The NF-kappaB-independent functions of IKK subunits in immunity and cancer. Trends Cell Biol 2009; 19:404-13; PMID:19648011; http://dx.doi.org/10.1016/j.tcb.2009.05.006
11. Comb WC, Cogswell P, Sitcheran R, Baldwin AS. IKK-dependent, NF-κB-independent control of autophagic gene expression. Oncogene 2011; 30:1727-32; PMID:21151171; http://dx.doi.org/10.1038/onc.2010.553
12. Kim JE, You DJ, Lee C, Ahn C, Seong JY, Hwang JI. Suppression of NF-kappaB signaling by KEAP1 regulation of IKKbeta activity through autophagic degradation and inhibition of phosphorylation. Cell Signal 2010; 22:1645-54; PMID:20600852; http://dx.doi.org/10.1016/j.cellsig.2010.06.004
13. Niida M, Tanaka M, Kamitani T. Downregulation of active IKK beta by Ro52-mediated autophagy. Mol Immunol 2010; 47:2378-87; PMID:20627395; http://dx.doi.org/10.1016/j.molimm.2010.05.004
14. Magnuson B, Ekim B, Fingar DC. Regulation and function of ribosomal protein S6 kinase (S6K) within mTOR signalling networks. Biochem J 2012; 441:1-21; PMID:22168436; http://dx.doi.org/10.1042/BJ20110892
15. Kwiatkowski DJ. Tuberous sclerosis: from tubers to mTOR. Ann Hum Genet 2003; 67:87-96; PMID:12556239; http://dx.doi.org/10.1046/j.1469-1809.2003.00012.x
16. Manning BD, Tee AR, Logsdon MN, Blenis J, Cantley LC. Identification of the tuberous sclerosis complex-2 tumor suppressor gene product tuberin as a target of the phosphoinositide 3-kinase/akt pathway. Mol Cell 2002; 10:151-62; PMID:12150915; http://dx.doi.org/10.1016/S1097-2765(02)00568-3
17. Inoki K, Li Y, Zhu T, Wu J, Guan KL. TSC2 is phosphorylated and inhibited by Akt and suppresses mTOR signalling. Nat Cell Biol 2002; 4:648-57; PMID:12172553; http://dx.doi.org/10.1038/ncb839
18. Urano J, Sato T, Matsuo T, Otsubo Y, Yamamoto M, Tamanoi F. Point mutations in TOR confer Rheb-independent growth in fission yeast and nutrient-independent mammalian TOR signaling in mammalian cells. Proc Natl Acad Sci U S A 2007; 104:3514-9; PMID:17360675; http://dx.doi.org/10.1073/pnas.0608510104
19. Sancak Y, Thoreen CC, Peterson TR, Lindquist RA, Kang SA, Spooner E, et al. PRAS40 is an insulin-regulated inhibitor of the mTORC1 protein kinase. Mol Cell 2007; 25:903-15; PMID:17386266; http://dx.doi.org/10.1016/j.molcel.2007.03.003
20. Kovacina KS, Park GY, Bae SS, Guzzetta AW, Schaefer E, Birnbaum MJ, et al. Identification of a proline-rich Akt substrate as a 14-3-3 binding partner. J Biol Chem 2003; 278:10189-94; PMID:12524439; http://dx.doi.org/10.1074/jbc.M210837200
21. Pierce JW, Schoenleber R, Jesmok G, Best J, Moore SA, Collins T, et al. Novel inhibitors of cytokine-induced IkappaBalpha phosphorylation and endothelial cell adhesion molecule expression show anti-inflammatory effects in vivo. J Biol Chem 1997; 272:21096-103; PMID:9261113; http://dx.doi.org/10.1074/jbc.272.34.21096
22. Geleziunas R, Ferrell S, Lin X, Mu Y, Cunningham ET Jr., Grant M, et al. Human T-cell leukemia virus type 1 Tax induction of NF-kappaB involves activation of the IkappaB kinase α (IKKalpha) and IKKbeta cellular kinases. Mol Cell Biol 1998; 18:5157-65; PMID:9710600
23. Nakano H, Shindo M, Sakon S, Nishinaka S, Mihara M, Yagita H, et al. Differential regulation of IkappaB kinase α and β by two upstream kinases, NF-kappaB-inducing kinase and mitogen-activated protein kinase/ERK kinase kinase-1. Proc Natl Acad Sci U S A 1998; 95:3537-42; PMID:9520401; http://dx.doi.org/10.1073/pnas.95.7.3537
24. Skaug B, Jiang X, Chen ZJ. The role of ubiquitin in NF-kappaB regulatory pathways. Annu Rev Biochem 2009; 78:769-96; PMID:19489733; http://dx.doi.org/10.1146/annurev.biochem.78.070907.102750
25. Brown K, Gerstberger S, Carlson L, Franzoso G, Siebenlist U. Control of I kappa B-alpha proteolysis by site-specific, signal-induced phosphorylation. Science 1995; 267:1485-8; PMID:7878466; http://dx.doi.org/10.1126/science.7878466
26. Kim C, Ye F, Ginsberg MH. Regulation of integrin activation. Annu Rev Cell Dev Biol 2011; 27:321-45; PMID:21663444; http://dx.doi.org/10.1146/annurev-cellbio-100109-104104
27. Ruoslahti E. RGD and other recognition sequences for integrins. Annu Rev Cell Dev Biol 1996; 12:697-715; PMID:8970741; http://dx.doi.org/10.1146/annurev.cellbio.12.1.697
28. Nishiuchi R, Takagi J, Hayashi M, Ido H, Yagi Y, Sanzen N, et al. Ligand-binding specificities of laminin-binding integrins: a comprehensive survey of laminin-integrin interactions using recombinant α3β1, α6β1, α7β1 and α6β4 integrins. Matrix Biol 2006; 25:189-97; PMID:16413178; http://dx.doi.org/10.1016/j.matbio.2005.12.001
29. Carter WG, Wayner EA, Bouchard TS, Kaur P. The role of integrins α 2 β 1 and α 3 β 1 in cell-cell and cell-substrate adhesion of human epidermal cells. J Cell Biol 1990; 110:1387-404; PMID:1691191; http://dx.doi.org/10.1083/jcb.110.4.1387
30. Werb Z, Tremble PM, Behrendtsen O, Crowley E, Damsky CH. Signal transduction through the fibronectin receptor induces collagenase and stromelysin gene expression. J Cell Biol 1989; 109:877-89; PMID:2547805; http://dx.doi.org/10.1083/jcb.109.2.877
31. Dedhar S, Jewell K, Rojiani M, Gray V. The receptor for the basement membrane glycoprotein entactin is the integrin α 3/β 1. J Biol Chem 1992; 267:18908-14; PMID:1527019
32. Egles C, Huet HA, Dogan F, Cho S, Dong S, Smith A, et al. Integrin-blocking antibodies delay keratinocyte re-epithelialization in a human three-dimensional wound healing model. PLoS One 2010; 5:e10528; PMID:20502640; http://dx.doi.org/10.1371/journal.pone.0010528
33. Debnath J, Mills KR, Collins NL, Reginato MJ, Muthuswamy SK, Brugge JS. The role of apoptosis in creating and maintaining luminal space within normal and oncogene-expressing mammary acini. Cell 2002; 111:29-40; PMID:12372298; http://dx.doi.org/10.1016/S0092-8674(02)01001-2
34. Debnath J, Muthuswamy SK, Brugge JS. Morphogenesis and oncogenesis of MCF-10A mammary epithelial acini grown in three-dimensional basement membrane cultures. Methods 2003; 30:256-68; PMID:12798140; http://dx.doi.org/10.1016/S1046-2023(03)00032-X
35. Jung CH, Ro SH, Cao J, Otto NM, Kim DH. mTOR regulation of autophagy. FEBS Lett 2010; 584:1287-95; PMID:20083114; http://dx.doi.org/10.1016/j.febslet.2010.01.017
36. Petiot A, Ogier-Denis E, Blommaart EF, Meijer AJ, Codogno P. Distinct classes of phosphatidylinositol 3'-kinases are involved in signaling pathways that control macroautophagy in HT-29 cells. J Biol Chem 2000; 275:992-8; PMID:10625637; http://dx.doi.org/10.1074/jbc.275.2.992
37. Degenhardt K, Mathew R, Beaudoin B, Bray K, Anderson D, Chen G, et al. Autophagy promotes tumor cell survival and restricts necrosis, inflammation, and tumorigenesis. Cancer Cell 2006; 10:51-64; PMID:16843265; http://dx.doi.org/10.1016/j.ccr.2006.06.001
38. Lock R, Roy S, Kenific CM, Su JS, Salas E, Ronen SM, et al. Autophagy facilitates glycolysis during Ras-mediated oncogenic transformation. Mol Biol Cell 2011; 22:165-78; PMID:21119005; http://dx.doi.org/10.1091/mbc.E10-06-0500
39. Dan HC, Baldwin AS. Differential involvement of IkappaB kinases α and β in cytokine- and insulin-induced mammalian target of rapamycin activation determined by Akt. J Immunol 2008; 180:7582-9; PMID:18490760
40. Karin M, Ben-Neriah Y. Phosphorylation meets ubiquitination: the control of NF-[κ]B activity. Annu Rev Immunol 2000; 18:621-63; PMID:10837071; http://dx.doi.org/10.1146/annurev.immunol.18.1.621

41. Friedland JC, Lakins JN, Kazanietz MG, Chernoff J, Boettiger D, Weaver VM. α6β4 integrin activates Rac-dependent p21-activated kinase 1 to drive NF-kappaB-dependent resistance to apoptosis in 3D mammary acini. J Cell Sci 2007; 120:3700-12; PMID:17911169; http://dx.doi.org/10.1242/jcs.03484
42. Weaver VM, Lelièvre S, Lakins JN, Chrenek MA, Jones JC, Giancotti F, et al. β4 integrin-dependent formation of polarized three-dimensional architecture confers resistance to apoptosis in normal and malignant mammary epithelium. Cancer Cell 2002; 2:205-16; PMID:12242153; http://dx.doi.org/10.1016/S1535-6108(02)00125-3
43. Scaife CL, Kuang J, Wills JC, Trowbridge DB, Gray P, Manning BM, et al. Nuclear factor kappaB inhibitors induce adhesion-dependent colon cancer apoptosis: implications for metastasis. Cancer Res 2002; 62:6870-8; PMID:12460901
44. Chen N, Eritja N, Lock R, Debnath J. Autophagy restricts proliferation driven by oncogenic phosphatidylinositol 3-kinase in three-dimensional culture. Oncogene 2012; PMID:22777351; http://dx.doi.org/10.1038/onc.2012.277
45. Gong C, Bauvy C, Tonelli G, Yue W, Deloménie C, Nicolas V, et al. Beclin 1 and autophagy are required for the tumorigenicity of breast cancer stem-like/progenitor cells. Oncogene 2013; 32:2261-72; PMID:22733132; http://dx.doi.org/10.1038/onc.2012.252
46. Debnath J, Walker SJ, Brugge JS. Akt activation disrupts mammary acinar architecture and enhances proliferation in an mTOR-dependent manner. J Cell Biol 2003; 163:315-26; PMID:14568991; http://dx.doi.org/10.1083/jcb.200304159
47. Debnath J. Detachment-induced autophagy in three-dimensional epithelial cell cultures. Methods Enzymol 2009; 452:423-39; PMID:19200896; http://dx.doi.org/10.1016/S0076-6879(08)03625-2